

Conformation and structural features of diuron and irgarol: insights from quantum chemistry calculations

Bouchouireb Zakaria ¹, Sussarellu Rossana ², Stachowski-Haberkorn Sabine ², Graton Jérôme ¹,
Le Questel Jean-Yves ^{1,*}

¹ Nantes Université, CNRS, CEISAM, UMR 6230, F-44000 Nantes, France

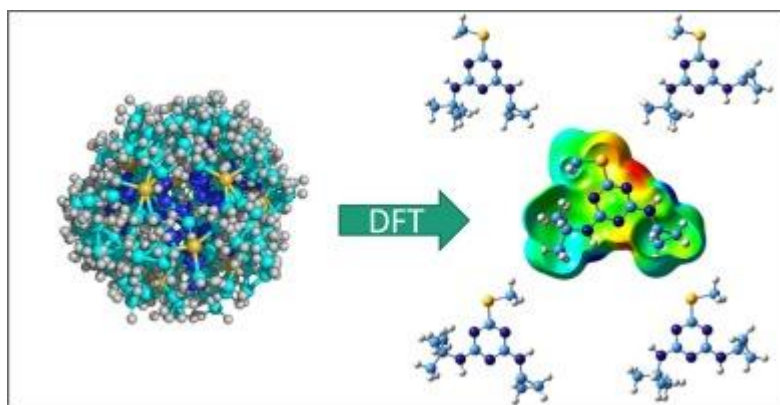
² Ifremer, BE-LEX, F-44300, Nantes, France

* Corresponding author : Jean-Yves Le Questel, email address : jean-yves.le-questel@univ-nantes.fr

Abstract :

The structure and the conformations of diuron and irgarol have been investigated from crystal structure analyses and Density Functional Theory (DFT) calculations. Significant changes in terms of conformer distribution are found according to the surroundings (gas phase or water). Irgarol appears expectedly as flexible from a conformational point of view, nine or eight conformers being identified in the isolated state and water, respectively. Natural Bond Orbital (NBO) analyses have been realised on the energetic minima to rationalise the conformational preferences. Molecular electrostatic potential calculations have been carried out to bring to light and rank the potential intermolecular interaction sites of the two biocides. The interaction potential of irgarol, essentially represented by the triazine nitrogen atoms and the NH groups, is found to be much more sensitive to the conformational preferences than the one of diuron, the N3 triazine being preferred as HB acceptor, in agreement with the crystallographic data available.

Graphical abstract



Highlights

► Diuron and irgarol structural features have been investigated by quantum chemistry (DFT) calculations and analyses of crystal structures retrieved from the Cambridge Structural Database (CSD) and the protein data bank (PDB). ► The effect of the surroundings have been taken into account in the calculations using the SMD model for water. ► Molecular electrostatic potential calculations allowed to bring to light and rank the potential intermolecular interaction sites of the two biocides according to their conformation. ► The potential of interaction of irgarol is found to be much more sensitive to the conformational preferences than the one of diuron.

Keywords : algaecides, photosystem II inhibitors, DFT calculations, Molecular electrostatic potential

1. Introduction

Diuron (**1**, 1-(3,4 dichlorophenyl)-3,3 dimethyl urea) and Irgarol (**2**, 2-methylthio-4-

Journal Pre-proofs

frequently used in the formulation of algicides found in antifouling coatings for marine applications. The ban on the use of TBT (Tributyltin) [[1]] partly explains their development and widespread use in European countries until recently. Indeed, their detection in the environment [[2]] at concentrations possibly harmful towards photosynthetic organisms [[3]] made them included in the list of “48 priority pollutants to be monitored in European waters” in the Water Framework Directive (2000/60/EC and 2013/39/EU), the objective being to impose their progressive prohibition over the next 20 years.

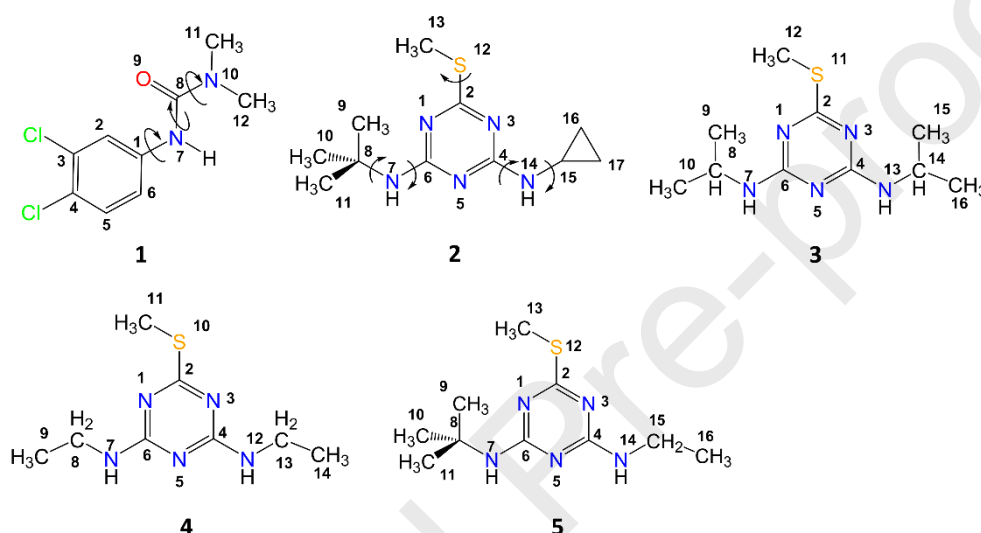


Figure 1. Chemical structure and numbering of diuron (**1**) irgarol (**2**) prometryn (**3**) symetryn (**4**) and terbutryn (**5**) herbicides. Generated with ChemDraw Professional (19.1.0.8, PerkinElmer Informatics, Inc.).

The activity of these biocides originates from their inhibition of the photosystem II (PSII) reaction core at the plastoquinone B (PLQ B) site of the D1 polypeptide center. More precisely, they compete with PLQ B at its binding site within the D1 protein, resulting in the displacement of PLQ B from its binding site, and a blocking of electron transfer [[4]]. Diuron **1** is a substituted aryl-urea whereas irgarol **2** is a substituted triazine, compounds of this family forming one of

the main chemical groups of PSII herbicides. Indeed, the class of aryl-ureas is often considered as the first of highly effective herbicides introduced in the sixties [[5]]. The understanding of

the binding interactions of such inhibitors with PSII is of interest for rationalizing their activity for the design of safe and efficient herbicides, but also for the understanding of their toxicity. In this context, comprehensive investigations on the conformational behavior and structural properties of the inhibitors are also important since flexible compounds such as druglike molecules adopt various conformations in solution, the solid state, and in different biological environments. In the case of these herbicides, earlier works have been published in the literature. Thus, the crystal structure of diuron has been resolved [[6]] and *ab initio* calculations have been performed at the Hartree-Fock level, the conformers energies being refined at the MP2 level [[7]]. More recently, the degradation mechanism of diuron in water has been investigated from molecular modeling through Density Functional Theory (DFT) calculations [[8]]. For irgarol, no crystal structure is available but structural data exist for related compounds such as prometryn **3** [[9], [10]] and symetrin **4** [[11]]. However, to our knowledge, no molecular modeling studies dedicated to irgarol have been carried out.

Recent studies have emphasized the importance of conformer generation in drug discovery, as well as in structure-based design than for the prediction of relevant drug properties (for example related to the ADMET drug profile: absorption, distribution, metabolism, excretion and toxicology) [12], [13]. In this quest for the most accurate description of the conformational landscape of bioligands, these studies have shown that DFT calculations, taking into account the influence of the surroundings, and the use of solid state informations, are among the best approaches. At the present time, new theoretical approaches such as the domain-based local pair-natural orbital coupled-cluster [DLPNO-CCSD(T)] method [14] have been shown to lead with a reasonable computational cost to accurate conformational energies for organic ligands such as small peptides and medium-size macrocycles [15]. Nevertheless, the M06-2X functional

remains widely used and is still considered as the most accurate for thermochemistry, kinetics, and noncovalent interactions.

features of diuron and irgarol (ii) gas phase and water (SMD continuum model) M06-2X DFT calculations to investigate the conformational preferences of the two biocides in various surroundings (iii) NBO analyses to rationalize the various trends and (iv) molecular electrostatic potential (MEP) calculations to highlight their interaction sites. Our work allows the identification of the main conformers of the two molecules, their energetic distribution, provides a ranking of their potential interaction sites according to their conformation and some leads to explain the predicted conformational preferences.

2. Material and Methods - Quantum chemistry calculations

The DFT calculations were carried out with the Gaussian16 program [16]. The conformational analysis of diuron and irgarol was performed with the M06-2X functional [17] in combination with the triple-zeta 6-311++G(d,p) basis set. Rigid scans along the various rotatable bonds of diuron (C₁-N₇ see Figure 1) and irgarol (C₂-S₁₂, C₄-N₁₄, N₁₄-C₁₅, C₆-N₇, N₇-C₈ Figure 1) have systematically been conducted at the M06-2X/6-31++G(d,p) level in the isolated state and the water implicit solvation model. The solvent effect of water was taken into account using the SMD solvation continuum model [18]. Full geometry optimization followed by vibrational spectrum calculation for each low energy conformer was computed to confirm its nature of true minimum at the M06-2X/6-311++G(d,p) level, in the isolated state and water. Natural Bond Orbital analyses [19], using NBO version 3, were carried out on the various energetic minima of diuron and irgarol in the gas phase and the SMD water model in order to rationalize the conformational preferences. To identify potential intermolecular interaction sites of diuron and irgarol, several molecular electrostatic potential based descriptors were tested and

computed at the M6-2X/6-311++G(d,p) level. Thus, electrostatic potential values were calculated for HB donors (i) at a distance of 0.55 Å, according to the definition of $V_{\alpha}(r)$, from the α th hydrogen atom of the α th donor bond, as suggested by Kowalski [20], and (ii) at the electronic isodensity surface of 0.001 e bohr⁻³, corresponding to $V_{S,\max}$, as recommended by Bader [21]. The relative population of the various conformers was evaluated from the computed Gibbs energies through a Boltzmann distribution (Eq. (1)) and the theoretical descriptors weighted by these populations.

$$p_i = \frac{e^{-\Delta G_i / RT}}{\sum_{i=1}^n e^{-\Delta G_i / RT}} \quad (1)$$

3. Results

3.1 Structural database analyses.

3.1.1 Molecular structure

In this section, we discuss the conformational features of experimental structures of diuron and irgarol and relevant derivatives found in structural databases. We have first searched the Cambridge Structural Database (CSD) [22] mainly for diuron, prometryn and symetrin. In the case of terbutryn, no data were found in the CSD. We turned then to the Protein data Bank (PDB) [23]. In this framework, we remind the reader that the ligands obtained from PDB structures have much lower accuracy than the “small molecules” from the CSD. For this reason, one has to be cautious in the comparisons and analyses involving this data.

Figure 2 shows the molecular structure of diuron in the crystalline state (CLPHUR refcode, [6]) and Table S1 reports selected values of torsion angles on the basis of the numbering of the

Journal Pre-proofs

atoms specified in Figure 1. We have also used in Table S1 in a case of clarity the convention published by Kyne and Prelog in their seminal paper [24], and recommended by the IUPAC for

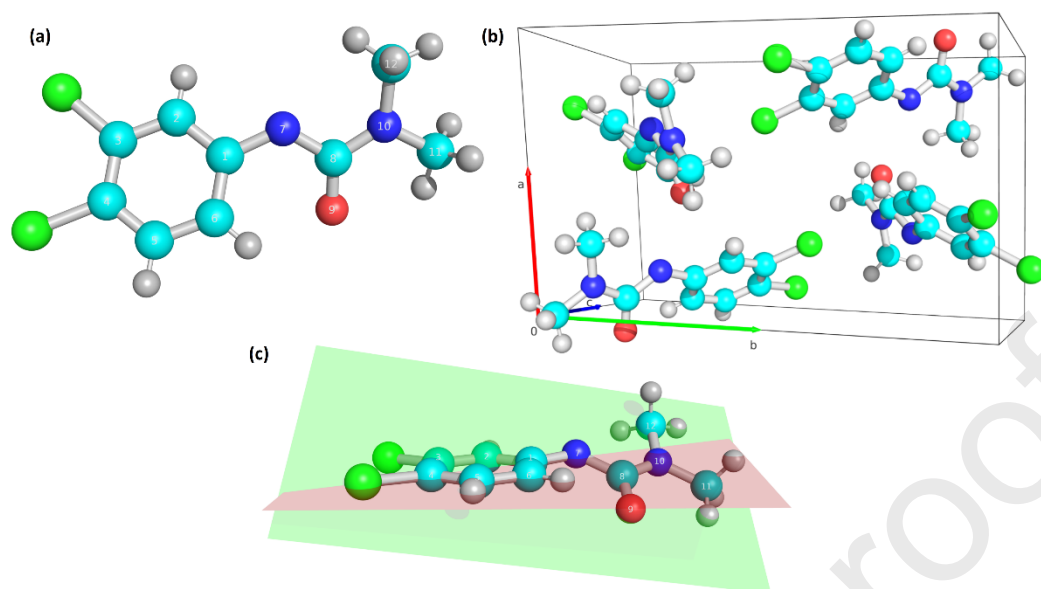


Figure 2. a) Molecular conformation of diuron in the solid state (CLPHUR refcode [6]) b) A view of the unit cell c) View of the structure showing the two planes in the molecule and their relative orientation. The orange plane refers to the aromatic ring while the green one refers to the urea group). Generated with PyMOL (The PyMOL Molecular Graphics System, Version 2.5a Schrödinger, LLC).

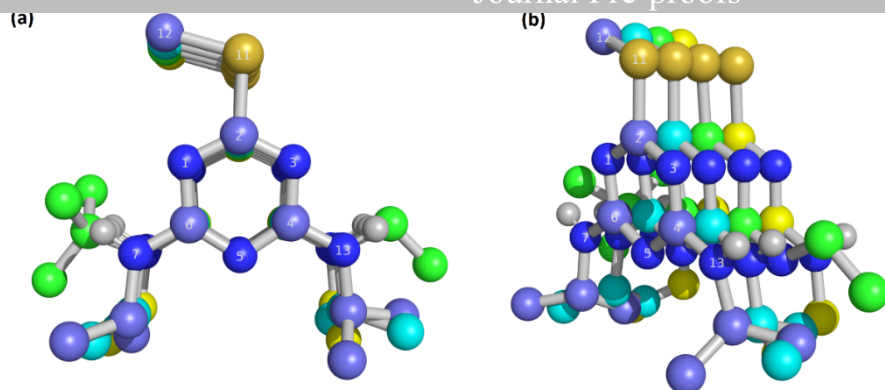
the torsion angles. Of course, one has to keep in mind that differences of torsion angles less than 30° do not generally represent significant differences in terms of conformational landscape. The solid state structure of the diuron molecule presents two planes, one containing the aromatic ring, the other the urea group. These two planes form between them an angle of 30° . The urea group is in a *transoid* conformation (carbonyl group with respect to the NH group).

No structure of irgarol is found in the Cambridge Structural Database (CSD) [22]. However, atomic coordinates are available for herbicides belonging to the same triazine chemical family. Thus, the orientation of the S-C single bond is very similar in the various entries, being syn-periplanar (*sp*) and quasi-planar to the triazine ring. The conformation of the lateral chains

shows more conformational freedom. As such, it is identical (*sp*), and almost in the plane of the aromatic ring, in the case of prometryn and symetryn (values of about 5°) for the N5-C6-N7-C8

torsion angle. In contrast, in the case of terbutryn, it is anti-periplanar (*ap*) in all three co-crystals

Journal Pre-proofs



(1DXR 2BNP, 2BNS entries) [25], [26] found in the protein data bank (PDB) [23]. For the N5-C4-N-C torsion angle, an *sp* orientation is observed in prometryn, symetryn (DADDIV01 CSD refcode) [9], [10] and symetryn (EAMTTE refcode) [11], whereas the corresponding torsion angle ranges in terbutryn in protein surroundings are typical of an *ap* orientation. Table S1 shows that the C4-N-C-C and C6-N7-C8-C torsion angles show even more conformational flexibility, since, according to the entry, the orientation can be quite different: *ap* and *ac* for C4-N-C-C and *ap*, *sc* or *ac* for C6-N7-C8-C. Figure 3 shows the superposition of the various triazine derivatives on the triazine and thiomethyl moieties (8 atoms) while considering prometryn (DADDIV01) as the reference structure. This Figure illustrates the conservation of the same orientation of the thiomethyl group in the various structures. In contrast, it appears clearly from Figure 3 that the lateral chains attached on the C4 and C6 carbon atoms of the triazine ring can adopt different conformations, in line with the above analysis of the torsional angles (Table S1).

Figure 3. (a) (b) Molecular fitting of the various triazine derivatives showing the different conformations of the lateral chains of the triazine ring. The carbon atoms of the various structures have been colored differently to better identify them (reference structure: prometryn (DADDIV01 [9,10]) in blue; second independent molecule of the DADDIV01 unit cell, in purple; symetryn (EAMTTE [11]) in yellow; terbutryn (in the 1DXR [21] PDB entry) in green. Generated with PyMOL (The PyMOL Molecular Graphics System, Version 2.5a Schrödinger, LLC).

Table 1 reports the values of geometric parameters of relevant interactions occurring in the various compounds and Figure 4 shows relevant molecular interactions.

Table 1. Geometric parameters (distances in Å and valence angles in °) of intermolecular interactions observed in the crystal structures of diuron and herbicide triazine derivatives. The CSD [20] (or PDB [23]) refcodes are indicated.

Compound/CSD (PDB) name	D-H...A	d(H...A)	θ (DH...A)	ϕ (H...AY)
<i>Diuron</i>				
CLPHUR02	N ₇ H...O ₉	1.96	157	139
	C ₂ H...O ₉	2.48	127	155
	C ₁₁ H...O ₉	2.42	128	101
<i>Prometryn</i>				
DADDIV01	N' ₇ H...N ₁	2.21	173	125
	N ₇ H...N' ₁	2.26	165	126
	N' ₁₄ H...N ₃	2.28	177	127
	N ₁₄ H...N' ₃	2.19	173	112
<i>Symetrin</i>				
EAMTTE	N ₁₂ H...N ₃	2.09	167	126
	N ₇ H...N ₅	2.48	134	103
<i>terbutryn</i>				

1DXR	OHw...N ₃	2.1	167	126
	N ₇ H...OC(Tyr222)	2.4	158	129

Journal Pre-proofs

	NH(Ile224)...N ₅	2.1	167	126
2BNP	N ₇ H...OC(Tyr222)	2.7	163	125
	N ₁₄ H...O γ (Ser223)	2.2	130	136
	NH(Ile224)...N ₅	2.2	155	111
2BNS	N ₇ H...OC(Tyr222)	2.7	157	124
	N ₁₄ H...O γ (Ser223)	2.2	133	130
	NH(Ile224)...N ₅	2.2	149	112

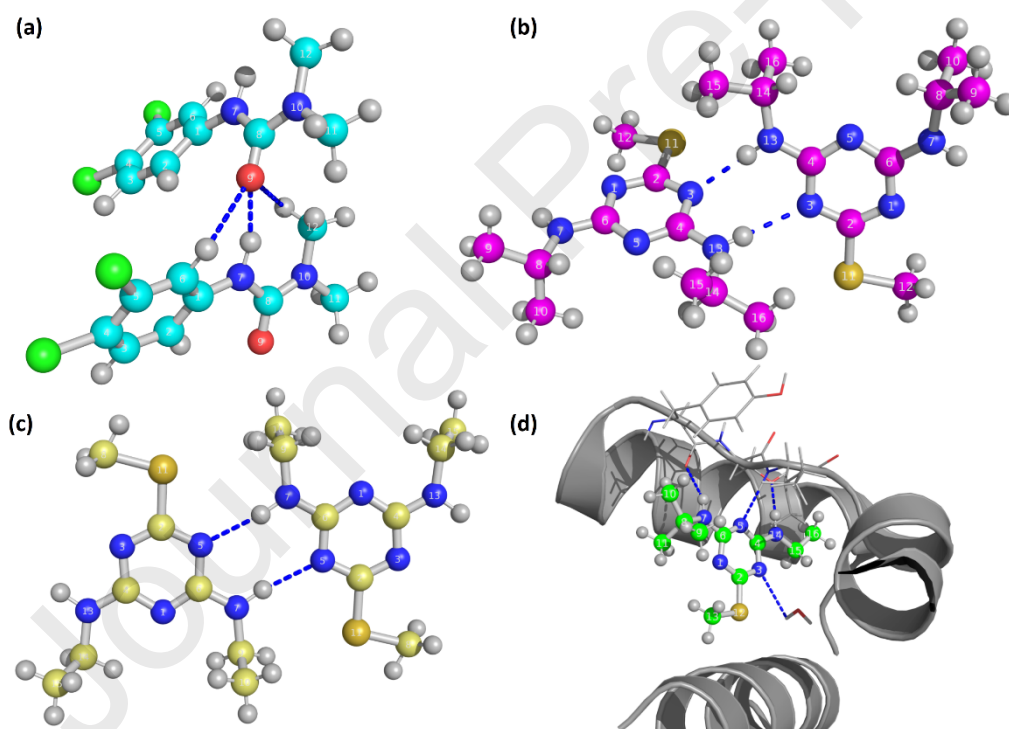


Figure 4. HB distances (blue dashes) observed in CSD crystal structures of a) diuron (CIPHUR02 [6]) b) prometryn (DADDIV01 [9,10]) c) symetrin (EAMTTE [11]) and d) in

protein surroundings for terbutryn (1DXR [21]). Generated with PyMOL (The PyMOL Molecular Graphics System, Version 2.5a Schrödinger, LLC).

Thus, in the case of diuron, the main Hydrogen-bond (HB) interactions sites are involved in the crystal packing of the observed solid-state conformation. The carbonyl oxygen is the main HB acceptor while the polarized CH groups (an aromatic CH (C₆H) close to the chlorine atoms and an alkyl CH (C₁₂H) carried by the nitrogen of the amide moiety, Figure 4a)) are involved as HB donors, the corresponding d(H...O) being significantly smaller than the sum of the Van der Waals radii (2.72 Å). The shortest HB is observed for the NH...O interaction, which also appears more linear and more directional compared to the (C)H...OC HB when the valence angles DH...A and H...AY of the corresponding interactions are taken into account. Indeed, as recommended by Desiraju and Steiner in their monograph [27], the consideration of HB angles, not only of HB lengths, are important when comparing HB features involving weak HB.

In the case of the triazine derivatives, significant differences are observed among the various compounds. Thus, in CSD entries, in the prometryn structure (DADDIV01 [9,10]), only the N₅ triazine nitrogen is not involved in any HB interaction, chains extending along the b crystallographic axis and involving N₇H...N₁ and N₁₃H...N₃ interactions being observed (Figure 4b). This is not the case in the symetrin crystallographic structure (EAMTTE refcode [11]) in which a HB N₁₃H...N₃ dimer is observed, the HB donating potential of the N₇H fragment being used in a N₇H...N₅ interaction (Figure 4c).

Lastly, it is interesting to note that in protein environments (1DXR [21], 2BNP, 2BNS [22]), the various HB interactions are conserved in the three PDB entries (see Table 1). We have shown the HB network on Figure 4d on the example of 1DXR, this entry having the best resolution (2.00 Å) among the three x-ray structures. Thus, in the case of 1DXR [21], a HB involving the N₃ sp² nitrogen of the triazine ring of terbutryn as an acceptor is observed with a water molecule, whereas in the two other PDB entries (2BNP and 2BNS [22]) no water

molecule is found in this area. The low Root Mean Square Deviation (RMSD) values of the fittings of 2BNP (0.499 Å) and BNS (0.514 Å) taking as reference the 1DNX structure and

considering the Clusters illustrate the conservation of structure and interactions in the receptor surroundings. It appears that in the protein environment, the terbutryn molecule uses much more its HB potential since only the N₁ nitrogen of the triazine ring is not involved in any HB.

3.2 DFT calculations.

3.2.1 Conformer distribution

Table 2 and Table 3 respectively report the distribution of the conformers of diuron and irgarol computed at the M06-2X/6-311+G(d,p) level of theory in the isolated state and in the water SMD model.

Table 2. Conformational distribution of the energetic minima of diuron computed at the M06-2X/6-311+G(d,p) level in the isolated state and in the SMD water model.

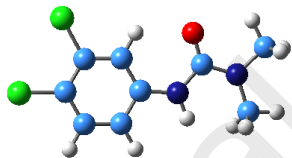
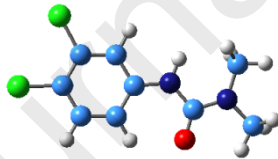
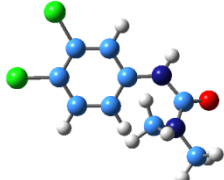
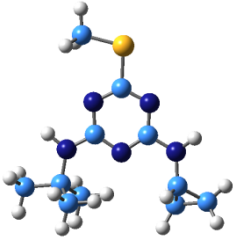
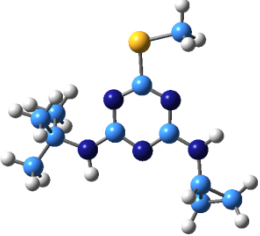
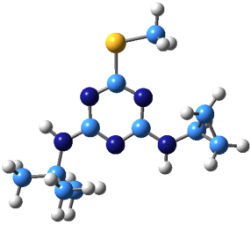
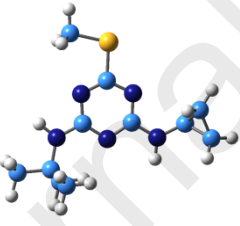
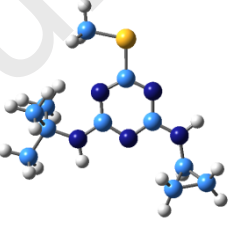
Conformer	3D structure	Isolated state		Water	
		ΔG (kJ/mol)	p_i (%)	ΔG (kJ/mol)	p_i (%)
D1		0.0	54	0.0	67
D2		0.6	42	2.2	33
D3		7.9	2	8.8	<0.2

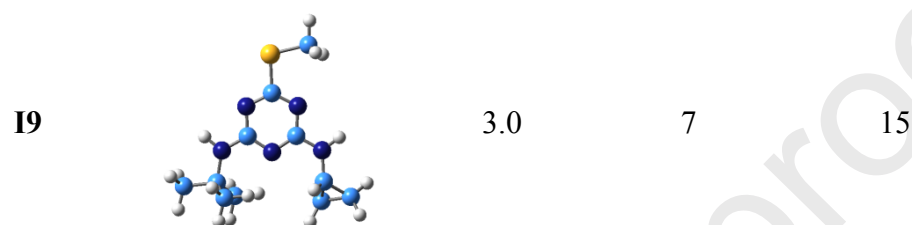
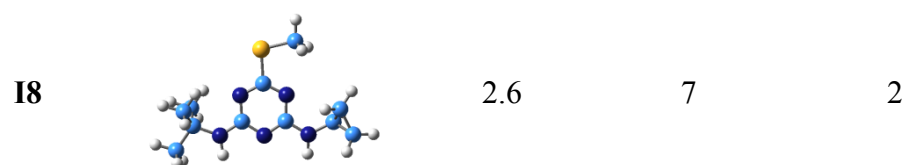
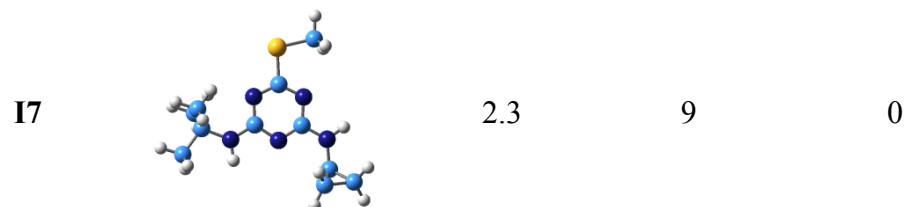
Table 3. Conformational distribution of the energetic minima of irgarol computed at the M06-2X/6-311+G(d,p) level in the isolated state and in the SMD water model. Only the percentage

Journal Pre-proofs

Conformer	3D structure	Isolated state		Water
		ΔG (kJ/mol)	p_i (%)	p_i (%)
I1		0.0	19	16
I2		0.3	17	8
I3		0.4	16	7
I4		1.7	10	6
I5		1.9	9	37



Journal Pre-proofs



3.2.2 NBO analyses

Table 4 and Table 5 respectively report the second order perturbation energies E^2_{ij} calculated at the M06-2X/6-311+G(d,p) level for the various energetic minima of diuron and irgarol in the isolated state and in the water SMD model. Complementary informations from these analyses (NBO occupancy and orbital energy) are given in Table S2 and S3 of the Supplementary Materials for the two compounds.

Table 4. Second order perturbation energies E^2_{ij} (kcal/mol) calculated at the M06-2X/6-311+G(d,p) level for the various energetic minima of diuron a) in the isolated state and b) in the water SMD model.

a)

Donor	Acceptor	D1	D2	D3
		E^2_{ij}	E^2_{ij}	E^2_{ij}
LP N7	π^*C1-C2	40.7	38.8	25.8
	σ^*C8-O9	33.6	42.5	2.2

	π^*C8-O9	6.6	3.7	43.4
LP1 O8	$\sigma^*C2-H/C6-H$	1.1	0.9	-
	σ^*N7-C8	1.7	1.7	1.6
	$\sigma^*C8-N10$	1.4	1.4	1.6
Journal Pre-proofs				
LP2 O8	$\sigma^*C2-H/C6-H$	1.2	0.1	-
	σ^*N7-C8	30.2	30.2	30.1
	$\sigma^*C8-N10$	28.1	28.0	28.1
	σ^*C11-H	0.52	0.59	0.6
LP N10	σ^*C8-O9	41.3	50.0	1.3
	π^*C8-O9	6.0	3.7	69.4
	σ^*C11-H'	7.6	7.4	8.1
	σ^*C11-H''	4.1	4.4	2.7
	σ^*C12-H	8.0	8.2	7.2

b)

Donor	Acceptor	D1a	D2a
		E^2_{ij}	E^2_{ij}
LP N7	$\pi^*C1-C2/C1-C6$	37.4	42.1
	σ^*C8-O9	-	-
	π^*C8-O9	-	-
LP1 O8	$\sigma^*C2-H/C6-H$	-	0.6
	σ^*N7-C8	1.5	1.5
	$\sigma^*C8-N10$	1.3	1.2
	$\sigma^*N10-C11$	0.5	0.6
LP2 O8	$\sigma^*C2-H/C6-H$	-	0.8
	σ^*N7-C8	26.6	26.4
	$\sigma^*C8-N10$	24.2	24.3
	σ^*C11-H	0.5	0.7
LP N10	σ^*C8-O9	-	-
	π^*C8-O9	-	-
	σ^*C11-H'	7.5	7.5
	σ^*C11-H''	1.7	1.3
	σ^*C12-H	7.6	7.1
	σ^*C12-H'	-	4.1

Table 5. Second order perturbation energies E^2_{ij} (kcal/mol) calculated at the M06-2X/6-311+G(d,p) level for the various energetic minima of irgarol a) in the isolated state and b) in the water SMD model.

a)

Donor	Acceptor	I1	I2	I3	I4	I5	I6	I7	I8	I9
		E^2_{ij}	E^2_{ij}	E^2_{ij}	E^2_{ij}	E^2_{ij}	E^2_{ij}	E^2_{ij}	E^2_{ij}	E^2_{ij}
LP N1	σ^*C2-N3	13.6	14.2	14.6	13.9	13.3	13.7	14.2	14.4	14.4
	σ^*N5-C6	13.4	13.5	13.3	13.0	13.0	12.6	13.5	13.1	13.7
	σ^*C6-N7	4.1	4.0	4.2	4.0	4.0	4.0	4.0	3.9	4.2

	$\sigma^*C2-S12$	3.4	2.7	2.7	3.4	3.5	3.5	2.7	2.7	2.6
LP N3	$\sigma^* N1-C2$	14.1	13.9	13.4	14.1	14.6	14.6	13.9	13.9	13.3
	σ^*C2-	2.5	3.4	3.5	2.6	2.6	2.7	3.4	3.6	3.3
Journal Pre-proofs										
	σ^*C4-N5	14.0	13.1	13.4	13.9	13.4	13.2	13.1	12.8	13.7
	$\sigma^*C4-N14$	4.4	4.2	4.5	4.5	4.3	4.5	4.2	4.4	4.3
LP N5	$\sigma^*C4-N14$	4.5	4.4	4.3	4.2	4.3	4.2	4.4	4.3	4.6
	$\sigma^* N3-C4$	13.1	14.1	13.9	13.3	13.6	13.6	14.1	14.1	13.6
	$\sigma^* N1-C6$	13.6	13.4	13.1	13.7	13.9	13.9	13.4	13.3	13
	σ^*C6-N7	4	4	3.7	3.8	4.1	4.1	4.0	4.0	4.0
	σ^*C11-H	0.5	0.6	0.6	0.6	0.6	-	-	-	-
LP1 S7	$\sigma^* N1-C2/C2-N3$	4.8	4.9	4.8	4.9	4.8	4.9	4.9	4.8	4.8
LP2 S7	$\pi^* N1-C2/C2-N3$	34.7	34.7	33.4	35.0	33.0	34.9	34.7	34.6	34.6
	σ^*C13-H	4.6	4.6	4.7	4.6	4.6	4.7	4.6	4.7	4.5
	σ^*C13-H'	4.6	4.5	4.4	4.6	4.7	4.6	4.5	4.4	4.7
LP N7	$\pi^* N1-C6$	82.0	82.7	82.6	81.6	82.2	78.9	82.6	82.0	79.6
	$\sigma^*C8-C10$	6.1	6.3	6.3	6.3	6.3	6.3	6.3	6.4	6.0
	$\sigma^*C8-C11$	6.5	6.2	6.5	6.3	6.4	6.4	6.2	6.2	6.6
LP N14	$\pi^* N3-C4$	69.9	71.3	71.5	72.6	73.0	72.0	71.5	70.3	71.8
	$\sigma^*C15-C16$	5.2	5.3	5.1	5.3	5.7	5.1	5.4	5.2	5.2
	σ^*C15-H	9.7	9.5	9.5	9.4	9.4	9.5	9.5	9.6	9.6

b)

		I1	I2	I3	I4	I5	I6	I7	I8	I9
Donor	Acceptor	E^2_{ij}	E^2_{ij}	E^2_{ij}	E^2_{ij}	E^2_{ij}	E^2_{ij}	E^2_{ij}	E^2_{ij}	E^2_{ij}
LP N1	σ^*C2-N3	14.1	14.3	14.6	14.4	13.9	14.3	13.9	14.5	14.3
	$\sigma^* N5-C6$	12.9	13.2	12.6	12.5	12.9	12.5	12.8	12.8	13
	σ^*C6-N7	3.8	3.7	3.9	3.8	3.9	3.6	3.9	3.7	3.8
	$\sigma^*C2-S12$	3.3	2.6	2.5	3.4	3.6	3.9	3.6	2.7	2.4
LP N3	$\sigma^* N1-C2$	14.1	14.2	13.8	14	14.4	14.3	14.4	14.2	13.8
	$\sigma^*C2-S12$	2.3	3.2	3.4	2.4	1.4	2.4	2.4	3.4	3.2
	σ^*C4-N5	13.3	12.8	13	13.3	12.9	12.8	12.6	12.6	13.2
	$\sigma^*C4-N14$	4.0	4.0	4.2	4.2	4.0	4.1	4.0	4.2	3.9
LP N5	$\sigma^*C4-N14$	4.5	4.2	4.2	4.2	3.8	4.1	3.9	4.1	4.6
	$\sigma^* N3-C4$	13.5	14.1	14	13.7	13.7	13.8	13.7	14.1	13.8

	σ^* N1-C6	13.7	13.3	13.5	13.9	13.6	1.6	13.6	13.3	13.4
	σ^* C6-N7	4.0	3.8	3.6	3.7	3.8	3.9	3.9	3.9	3.9
	σ^* C11-H	0.5	0.6	-	-	-	-	-	-	-
LP1 S7	σ^* N1-C2	5.0	5.1	5.0	5.1	4.9	4.9	4.8	5.1	5.0
Journal Pre-proofs										
LP2 S7	π^* N1-C2 /C2-N3	55.7	54.1	52.7	54.1	52.8	54	52.5	54.2	55.7
	σ^* C13-H	4.5	4.5	4.4	4.5	4.4	4.5	4.4	4.5	4.5
	σ^* C13-H'	4.5	4.5	4.5	4.5	4.4	4.4	4.4	4.4	4.5
LP N7	π^* N1-C6 / N5-C6	91.4	91.3	90.4	91.1	92.2	89.4	91.6	90.4	88.5
	σ^* C8-C10	5.7	5.9	6	6	6	6.4	6	6	5.3
	σ^* C8-C11	6.3	6.2	6.2	6.1	6	5.7	6	6.2	6.7
LP N14	π^* N3-C4	81.8	84.2	85.4	84.7	83.3	83.5	87.2	82.7	83.6
	σ^* C15-C16	6.4	7.4	7.1	7.4	7.2	7.3	8.2	7	6.3
	σ^* C15-H	8.5	8.1	8.2	8.1	8.3	8.3	8.4	8.3	8.5
	σ^* C12-H	-	-	-	-	-	-	-	-	-

3.2.3 Molecular electrostatic potential calculations

Figure 5 shows the values of molecular electrostatic potential based descriptors ($V_{s,\min}$, and $V_{s,\max}$ and V_{α} , see methodology section) computed at the molecular surface for diuron for the two main conformers (**D1** and **D2** of Table 1) in the isolated state. The detailed values for the various conformations are reported in the Supplementary Materials (Table S2).

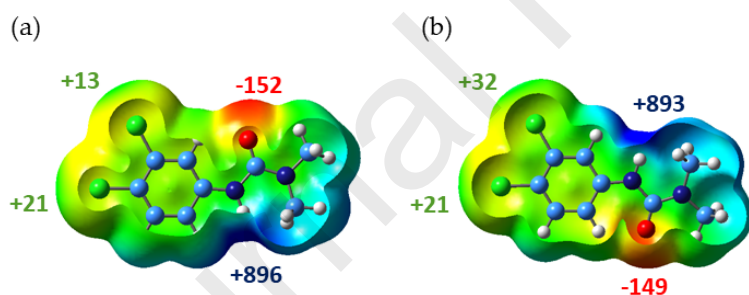


Figure 5. Molecular electrostatic potential descriptors computed at the molecular surface for the two diuron main conformers (**D1** (a) and **D2** (b)) at the M062X/6-311+G(d,p) level. Red areas correspond to electron rich regions, the value indicated in red corresponding to $V_{s,\min}$, the values indicated in green corresponding to $V_{s,\max}$. Finally, the number in blue corresponds to $V_{\alpha}(r)$.

The same descriptors are reported on Figure 6 for irgarol. Owing to the important conformational flexibility of this compound, the values of these descriptors have been weighted

Journal Pre-proofs

according to the area of each conformer and their corresponding population. The detailed values of the various descriptors for each conformation are reported in the Supplementary Materials (Table S3).

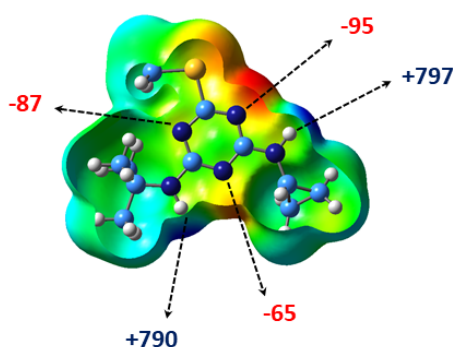


Figure 6. Molecular electrostatic potential descriptors computed at the molecular surface for one conformer (**15**) of irgarol at the M062X/6-311+G(d,p) level. Red areas correspond to electron rich regions, the value indicated in red corresponding to $V_{s,\min}$; the number in blue corresponds to V_{α} .

4. Discussion

4.1 Molecular Structure

The crystalline structures of diuron (CLPHUR and CLPHUR02 entries in the CSD) [6] show a *transoid* conformation of the urea fragment. The DFT calculations rationalize the observation of this conformation since they predict *cis* conformers to be at 8.8 kJ/mol (p_i of about 1%) above the minimum in the isolated state, this trend remaining true in the water continuum model, the corresponding conformer being separated of the absolute minimum from about 9 kJ/mol ($p_i \sim 0.2\%$) in water. In fact, in water, our calculations predict three families of conformers corresponding to the ones identified in the gas phase. Each family contains two to four conformers with similar torsion angles (differing from 5 to 30°). This is the reason why we have grouped the different conformers together according to their torsion angles, by summing their

population percentage. The minima found in our study are the same that those pointed out by Dos Santos *et al.* in their previous *ab initio* investigation [7]. However, a significant variation in their population is predicted at the DFT level, this trend being reinforced in the water continuum model in our results. In fact, in our results, conformer **D1** is favored (p_i of 54%), whereas in their study conformer **D2**, corresponding to the observed crystal conformation, had a slightly greater population (58% compared to 42% according to our calculations). Finally, it is worth noting that in their DFT investigation focused on the degradation of diuron in a SMD water model, Ren *et al.* only considered the most stable conformer (**D1** of Table 3) [8].

In the absence of any experimental structure, DFT calculations can be used to predict the various conformations of irgarol. The present results suggest therefore a high flexible conformational character for irgarol, nine conformations being possible, with populations ranging from 7 to 19 % in the isolated state and from 7 to 37 % in water (Table 4). A definitive answer on this behavior would be brought by *ab initio* molecular dynamics simulations. However, such investigations are beyond the scope of this manuscript. This behavior is in particular related to rotations around the lateral C_{ar} -N bonds carried by the triazine ring. Figure 3 indeed highlights this expected C_{ar} -N conformational flexibility from the fitting of crystal structures of irgarol analogs (prometryn, symetryn and terbutryn) whereas the 3D structures of its various conformers reported in Table 3 confirm this behavior. This Table also points out the flexibility around the C_{ar} -S bond, the influence of the surroundings being significant. Therefore, in the isolated state, the distribution of the various conformers is equilibrated, with about 50% for the two types of conformations (methyl group in the plane of the ring but either on the N_1 or the N_3 triazine atoms) whereas in water, the conformers *syn* to N_1 appear favored (they represent about 70% of the whole conformations).

4.2 NBO analyses

Table 4 shows that in the gas phase two main electronic effects are involved in the predilection of the two main *trans* conformers **D1** and **D2**. Thus, **D1** appears stabilized by strong conjugative electronic interactions between the N7 lone pair (100 % of p character) and the unoccupied antibonding C1=C2 orbital (LP N7 → π^* (C1=C2), 40.7 kcal/mol). It is worth noting that for the N7 lone pair, this delocalisation with the ring appears favoured over the one with the carbonyl C8=O9 bond LP N7 → π^* (C1=C2), 6.6 kcal/mol). The preference for this conformer is also due to strong hyperconjugative electronic interactions between (i) the lone pair of N7 and the unoccupied antibonding carbonyl C8C9 bond (LP N7 → σ^* (C8-C9), 33.6 kcal/mol) (ii) the lone pair of N10 (>98 % of p character) and the unoccupied antibonding carbonyl C8C9 bond (LP N10 → σ^* (C8-C9), 41.3 kcal/mol) (iii) one lone pair of the carbonyl oxygen (LP2 O8, 100 % of p-character) and the two unoccupied N-C (N7-C8 and C8-N10) orbitals (respective values of 30.2 and 28.1 kcal/mol for LP O8 → σ^* (N7-C8) and LP O8 → σ^* (C8-N10)). The stability of **D2** is rationalized by similar electronic effects. In the case of the minor **D3** conformer, the main electronic effects correspond to conjugative interactions of the N7 and N10 lone pairs with the unoccupied antibonding carbonyl C8=C9 bond : (LP N7 → π^* (C8=C9), 43.4 kcal/mol; LP N10 → π^* (C8=C9), 69.4 kcal/mol)). For this conformer, the other significant electronic interactions at work are conjugative interactions of the N7 lone pair with the aromatic ring (LP N7 → π^* (C1=C2), 25.8 kcal/mol) and hyperconjugative interactions with unoccupied antibonding C-H orbitals (LP N10 → σ^* (C11-H), LP N10 → σ^* (C12-H) with respective values of 8.1 and 7.2 kcal/mol).

The effect of the surrounding is significant since in water, the two previous main electronic effects are fewer and weaker. Thus, the N7 lone pair appears only involved in conjugative interactions with an antibonding orbital of the ring (LP N7 → π^* (C1=C2), 43.4 kcal/mol). The same is true for the N10 lone pair, which appears only involved in hyperconjugative interactions with unoccupied antibonding C-H orbitals (LP N10 → σ^* (C11-H), LP N10 → σ^* (C12-H) with

respective values of 7.5 and 7.6 kcal/mol in **D1** as an example, similar values being predicted for **D2**). This change of behaviour can be put in parallel with the less planar character of the amide moiety between the gas phase and water. Thus, the $\angle \text{C11N10C8O9}$ is close to 148° for the D1a and D2a conformers in water whereas the corresponding value is close to 7° in the gas phase.

In the case of irgarol, the NBO analysis points out (Table 5a) and 5b)) as the main electronic interactions stabilising the various conformers the ones involving the lone pairs of the heteroatoms connected to the triazine ring (N7, S12 and N14). These interactions are mainly conjugative ones and involve unoccupied antibonding π CN ring bonds. The most important in the gas phase appear the ones involving the N7 lone pair (100% of p-character $\text{LP N7} \rightarrow \pi^*$ (N1C6), range: 80 to 83 kcal/mol according to the conformers), followed by the ones involving the N14 lone pair (98 of p-character) $\text{LP N14} \rightarrow \pi^*$ (N3=C4), ranging from 70 to 73 kcal/mol depending on the conformations) and lastly by the second lone pair of S12 (100 % of p-character $\text{LP2 S12} \rightarrow \pi^*$ (N1=C2), close to 35 kcal/mol for all conformers). The other electronic effects involved in the 3D structure of the irgarol molecule concern the lone pairs of the cyclic nitrogen atoms (N1, N3 and N5) and correspond to hyperconjugative interactions with unoccupied σ CN antibonding orbitals of the triazine ring. Whatever the nitrogen lone pair involved, these interactions are characterized by close second order perturbation energies, ranging between 13 to 14 kcal/mol. The same trends in terms of electronic effects are predicted in the water SMD continuum model, both in terms of nature (conjugative and hyperconjugative) and of their amplitude, in contrast to the behaviour discussed previously for diuron.

4.3 Molecular Interactions

We have shown in previous studies the interest of molecular electrostatic potential quantum descriptors for the prediction of molecular interaction sites of organic molecules, including low molecular weight organic ligands of interest such as pesticides, and quantification of their HB

properties [28], [29], [30, 31]. Accordingly, to identify and analyze HB acceptors, absolute minima of the electrostatic potential (V_{\min}) or values computed on the molecular surface ($V_{s,\min}$),

Journal Pre-proofs

generally described by a 0.001 contour of electronic density, have been used in several studies to estimate HB strength, notably through correlation with experimental values from the pK_{BHX} database [32]. For HB donors, pioneering studies by Kenny have shown the interest of the $V_{\alpha}(r)$ descriptor [20], widely used for quantification of HB donating strength [[33, 34]].

Using these descriptors, the trends revealed by the DFT calculations for diuron are in line with the experimental observations, the oxygen atom of the urea group appearing as the main HB acceptor site. Oxygen atoms of urea carbonyl are classified as strong HB acceptors on the pK_{BHX} scale [32]. However, in the diuron molecule, the halogenated aromatic ring, through its strong electron-withdrawing effect, reduces the electron density at the carbonyl oxygen and therefore its HB accepting potential. From a HB donor point of view, the NH group of the urea moiety is logically pointed out as the best HB donor site. Figure 5 shows that this property is conformation dependent, variation of about 3 kJ/mol being predicted according to the conformer considered. It is thereby worth noting that the main conformer of diuron in the isolated state and water is shown to have the highest values of $V_{s,\min}$ and $V_{\alpha}(r)$, and therefore the best HB potential. It is also interesting to note that the chlorine atoms carried by the aromatic rings are identified as electrophilic sites from the calculations of the molecular electrostatic potential on the molecular surface. This property could be used in ligand-receptor interactions through halogen bonding, as it has been reported as an example for the lead compound of neonicotinoid insecticides, imidacloprid [35], with its ortho-chloropyridyl fragment, but also more generally in protein-ligand binding mechanisms [36].

In the case of irgarol, the values of $V_{s,\min}$ computed for the three triazine nitrogen atoms are significantly different, the most nucleophilic nitrogen corresponding to N_3 (Figure 6). The predicted range on the basis of $V_{s,\min}$ in terms of HB strength would therefore be the following:

$N_3 > N_1 > N_5$, the difference between N_3 and N_5 being of 30 kJ/mol whereas between N_3 and N_1 this difference amounts to 8 kJ/mol. However, it has been shown that triazine, compared to uridine, is a weak HB acceptor [22]. In the isolated molecule, this effect could partially be compensated by the electron-donating effect of the three substituents. In contrast, the values of the $V_\alpha(r)$ descriptor for the two NH groups differ of 7 kJ/mol, appearing therefore as comparable HB donor sites, less electrophilic than the diuron NH group. Table S2 in the Supplementary Materials shows that the variation of the $V_\alpha(r)$ values are negligible according to the change of conformation. These trends would have to be confirmed by deeper theoretical investigations, in particular based on the computations of energetic descriptors, but it is worth noting that among the three triazine nitrogen atoms, N_1 and N_5 do not use systematically their HB potential, whereas N_3 behaves as a HB acceptor in all crystal structures.

5. Conclusions

On the basis of the analysis of crystal structures found in the CSD and PDB databases and DFT quantum chemistry calculations, the geometrical features and the intermolecular interaction potential of diuron and irgarol, two biocides, have been investigated. The results of the theoretical calculations allow rationalizing the conformational preferences observed in the solid state. Quantum chemistry descriptors based on the molecular electrostatic potential allow to rank the various sites of molecular interactions in the two compounds. As a result, the carbonyl oxygen and NH groups of the urea moiety are found as the main HB sites of diuron and appear as strong HB acceptor and donor sites, respectively. Interestingly, this HB potential is found to be sensitive to the conformation. Furthermore, the potential of the chlorine atoms as halogen bond donors is pointed out. Irgarol is found to be flexible, nine or eight conformations being respectively identified in the isolated state and water, with a significant variation of the conformer populations according to the surroundings. From an intermolecular potential point

of view, the nitrogen atoms of the triazine ring are pointed out as HB acceptors, but with significantly different features. Thus, the N₃ nitrogen is highlighted to be the preferred acceptor,

in agreement with the HB observed in crystalline environments and one acceptor surroundings for relevant derivatives. In contrast, the HB donating strength of the NH groups is found to be less sensitive to the conformation. NBO analyses allow pointing out the main electronic effects (conjugative and hyperconjugative interactions) involved in the stabilisation of the various conformers of the two biocides according to the surroundings. The influence of the environment on the molecular structure and on these electronic effects appears more important in the case of diuron compared to irgarol. Indeed, the subtle distortion from planarity for diuron in water compared to the isolated state leads to fewer and weaker electronic effects than the ones occurring in the gas phase. This is not the case for irgarol, for which the trends remain similar in the gas phase and water, both in terms of electronic effects and amplitude.

On the whole, the present work shows, on the example of two biocides, how subtle chemical differences, mainly related to conformational features, can lead to significant changes in terms of HB properties that can have an impact on their behavior in molecular-recognition processes. Furthermore, it provides accurate geometries for use as reference or input structures in docking, molecular dynamics or QM/MM investigations aimed at an in-depth understanding of the binding of diuron and irgarol to their biological target.

Acknowledgements.

The CCIPL (Centre de Calcul Intensif des Pays de Loire) is acknowledged for provision of computer time. The authors declare no conflict of interest.

Author contributions

Conceptualization, J.-Y.L.Q., J.G., R.S. and S.S-H., methodology, J.-Y.L.Q. and J.G.; formal analysis, J.-Y.L.Q. and J.G; investigation, J.G. and Z.B., writing—original draft preparation,

J.G., J.-Y.L.Q.; writing—review and editing, J.-Y.L.Q., J.G., R.S., S.S-H., Z.B.; supervision, J.-Y.L.Q. and J.G., project administration, R.S. and S.S-H.; funding acquisition, R.S. and S.S-

H. All authors have read and agreed to the published version of the manuscript.

Journal Pre-proofs

Funding.

This research was funded by the IFREMER Institute, within the EMIHP project.

Supplementary material.

Complementary informations (torsion angles of the crystallographic structures analysed, NBO occupancy and orbital energy and minima and maxima of the molecular electrostatic potential on the molecular surface for the various conformations of diuron and irgarol) are provided in the supplementary material file. The three dimensional structures, optimised at the M062X/6-311+G(d,p) level, of the various minima of diuron and irgarol in the gas phase and water are available as a Zenodo dataset.

References

1. Manzo, S.; Buono, S.; Cremisini, C., Toxic Effects of Irgarol and Diuron on Sea Urchin *Paracentrotus lividus* Early Development, Fertilization, and Offspring Quality. *Archives of Environmental Contamination and Toxicology* **2006**, 51, (1), 61-68.
2. Caquet, T.; Roucaute, M.; Mazzella, N.; Delmas, F.; Madigou, C.; Farcy, E.; Burgeot, T.; Allenou, J. P.; Gabellec, R., Risk assessment of herbicides and booster biocides along estuarine continuums in the Bay of Vilaine area (Brittany, France). *Environmental Science and Pollution Research* **2013**, 20, (2), 651-666.
3. Dupraz, V.; Stachowski-Haberkorn, S.; Ménard, D.; Limon, G.; Akcha, F.; Budzinski, H.; Cedergreen, N., Combined effects of antifouling biocides on the growth of three marine microalgal species. *Chemosphere* **2018**, 209, 801-814.
4. Nelson, N.; Yocum, C. F., Structure and function of photosystems I and II. *Annual Review of Plant Biology* **2006**, 57, (1), 521-565.
5. Draber, W.; Tietjen, K.; Kluth, J. F.; Trebst, A., Herbicides in Photosynthesis Research. *Angewandte Chemie International Edition in English* **1991**, 30, (12), 1621-1633.
6. Pfefer, G.; Boistelle, R., Experimental and theoretical morphologies of diuron, N'-(3,4-dichlorophenyl)-N,N-dimethylurea. *Acta Crystallographica Section B* **1996**, 52, (4), 662-667.
7. Dos Santos, H. F.; O'Malley, P. J.; De Almeida, W. B., Gas phase and water solution conformational analysis of the herbicide diuron (DCMU): an ab initio study. *Theoretical Chemistry Accounts* **1998**, 99, (5), 301-311.
8. Ren, X.; Cui, Z.; Sun, Y., Theoretical studies on degradation mechanism for OH-initiated reactions with diuron in water system. *Journal of Molecular Modeling* **2014**, 20, (7), 2280.

9. Avey, H. P.; Kennard, C. H. L.; Smith, G., N,N'-Bis(1-methylethyl)-6-methylthio-1,3,5-triazine-2,4-diamine, prometryn, C₁₀H₁₉N₅S. *Acta Crystallographica Section C* **1985**, 41, (6), 938-940.
10. Lynch, D.; Smith, G.; Byriel, K.; Kennard, C., Molecular Cocrystals of Carboxylic Acids. VII. Structures of the 1:1 Adducts of 4-Nitrobenzoic Acid and 2,5-Dimethylthio-1,3,5-Triazine with N,N'-Bis(1-methylethyl)-6-methylthio-1,3,5-triazine-2,4-diamine (Prometryn). *Australian Journal of Chemistry* **1993**, 46, (6), 921-927.
11. Graham, A. J. A., D.; Sheldrick, B., 2,4-Bis(ethylamino)-6-methylthio-s-triazine (simetryne), C₈H₁₅N₅S. *Crystal Structure Communications* **1978**, 7, (2), 227-232
12. Hawkins, P. C. D., Conformation Generation: The State of the Art. *Journal of Chemical Information and Modeling* **2017**, 57, (8), 1747-1756.
13. Cavasin, A. T.; Hillisch, A.; Uellendahl, F.; Schneckener, S.; Göller, A. H., Reliable and Performant Identification of Low-Energy Conformers in the Gas Phase and Water. *Journal of Chemical Information and Modeling* **2018**, 58, (5), 1005-1020.
14. Sparta, M.; Neese, F., Chemical applications carried out by local pair natural orbital based coupled-cluster methods. *Chemical Society Reviews* **2014**, 43, (14), 5032-5041.
15. Rezac, J.; Bim, D.; Gutten, O.; Rulisek, L., Toward Accurate Conformational Energies of Smaller Peptides and Medium-Sized Macrocycles: MPCONF196 Benchmark Energy Data Set. *Journal of Chemical Theory and Computation* **2018**, 14, (3), 1254-1266.
16. Frisch, M. J.; Trucks, G. W.; Schlegel, H. B.; Scuseria, G. E.; Robb, M. A.; Cheeseman, J. R.; Scalmani, G.; Barone, V.; Petersson, G. A.; Nakatsuji, H.; Li, X.; Caricato, M.; Marenich, A. V.; Bloino, J.; Janesko, B. G.; Gomperts, R.; Mennucci, B.; Hratchian, H. P.; Ortiz, J. V.; Izmaylov, A. F.; Sonnenberg, J. L.; Williams, Ding, F.; Lipparini, F.; Egidi, F.; Goings, J.; Peng, B.; Petrone, A.; Henderson, T.; Ranasinghe, D.; Zakrzewski, V. G.; Gao, J.; Rega, N.; Zheng, G.; Liang, W.; Hada, M.; Ehara, M.; Toyota, K.; Fukuda, R.; Hasegawa, J.; Ishida, M.; Nakajima, T.; Honda, Y.; Kitao, O.; Nakai, H.; Vreven, T.; Throssell, K.; Montgomery Jr., J. A.; Peralta, J. E.; Ogliaro, F.; Bearpark, M. J.; Heyd, J. J.; Brothers, E. N.; Kudin, K. N.; Staroverov, V. N.; Keith, T. A.; Kobayashi, R.; Normand, J.; Raghavachari, K.; Rendell, A. P.; Burant, J. C.; Iyengar, S. S.; Tomasi, J.; Cossi, M.; Millam, J. M.; Klene, M.; Adamo, C.; Cammi, R.; Ochterski, J. W.; Martin, R. L.; Morokuma, K.; Farkas, O.; Foresman, J. B.; Fox, D. J. *Gaussian 16 Rev. B.01*, Wallingford, CT, 2016.
17. Zhao, Y.; Truhlar, D. G., The M06 suite of density functionals for main group thermochemistry, thermochemical kinetics, noncovalent interactions, excited states, and transition elements: two new functionals and systematic testing of four M06-class functionals and 12 other functionals. *Theoretical Chemistry Accounts* **2008**, 120, (1-3), 215-241.
18. Marenich, A. V.; Cramer, C. J.; Truhlar, D. G., Universal Solvation Model Based on Solute Electron Density and on a Continuum Model of the Solvent Defined by the Bulk Dielectric Constant and Atomic Surface Tensions. *Journal of Physical Chemistry B* **2009**, 113, (18), 6378-6396.
19. Reed, A. E.; Curtiss, L. A.; Weinhold, F., Intermolecular interactions from a natural bond orbital, donor-acceptor viewpoint. *Chemical Reviews* **1988**, 88, (6), 899-926.
20. Kenny, P. W., Hydrogen Bonding, Electrostatic Potential, and Molecular Design. *J. Chem. Inf. Model.* **2009**, 49, (5), 1234-1244.
21. Richard F. W. Bader, M. T. C., James R. Cheeseman, and Cheng Chang, Properties of atoms in molecules: atomic volumes. *J. Am. Chem. Soc.* **1987**, 109, (26), 7968-7979.
22. Groom, C. R.; Bruno, I. J.; Lightfoot, M. P.; Ward, S. C., The Cambridge Structural Database. *Acta Crystallographica Section B* **2016**, 72, (2), 171-179.

23. Berman, H. M.; Westbrook, J.; Feng, Z.; Gilliland, G.; Bhat, T. N.; Weissig, H.; Shindyalov, I. N.; Bourne, P. E., The Protein Data Bank. *Nucleic Acids Research* **2000**, 28, (1), 235-242.
24. Klyne, W.; Prelog, V., Description of steric relationships across single bonds. *Experientia* **1960**, 16, (12), 521-522.
25. Lancaster, C. R. D.; Dibikova, M. V.; Sabatino, F.; Ocstenich, D.; Michel, H., Structural Basis of the Drastically Increased Initial Electron Transfer Rate in the Reaction Center from a *Rhodospseudomonas viridis* Mutant Described at 2.00-Å Resolution *. *Journal of Biological Chemistry* **2000**, 275, (50), 39364-39368.
26. Katona, G.; Snijder, A.; Gourdon, P.; Andréasson, U.; Hansson, Ö.; Andréasson, L.-E.; Neutze, R., Conformational regulation of charge recombination reactions in a photosynthetic bacterial reaction center. *Nature Structural & Molecular Biology* **2005**, 12, (7), 630-631.
27. Desiraju, G.; Steiner, T., *The Weak Hydrogen Bond: Applications to Structural Chemistry and Biology*. 1999; p 528 pp.
28. Laurence, C.; Graton, J.; Berthelot, M.; Besseau, F.; Le Questel, J.-Y.; Lucon, M.; Ouvrard, C.; Planchat, A.; Renault, E., An Enthalpic Scale of Hydrogen-Bond Basicity. 4. Carbon pi Bases, Oxygen Bases, and Miscellaneous Second-Row, Third-Row, and Fourth-Row Bases and a Survey of the 4-Fluorophenol Affinity Scale. *Journal of Organic Chemistry* **2010**, 75, (12), 4105-4123.
29. Taillebois, E.; Alamiddine, Z.; Brazier, C.; Graton, J.; Laurent, A. D.; Thany, S. H.; Le Questel, J.-Y., Molecular features and toxicological properties of four common pesticides, acetamiprid, deltamethrin, chlorpyrifos and fipronil. *Bioorganic & Medicinal Chemistry* **2015**, 23, 1540-1550.
30. Graton, J. r. m.; Le Questel, J.-Y.; Maxwell, P.; Popelier, P., Hydrogen-Bond Accepting Properties of New Heteroaromatic Ring Chemical Motifs: A Theoretical Study. *Journal of Chemical Information and Modeling* **2016**, 56, (2), 322-334.
31. Alamiddine, Z.; Thany, S.; Graton, J.; Le Questel, J. Y., Conformations and Binding Properties of Thiametoxam and Clothianidin Neonicotinoid Insecticides to Nicotinic Acetylcholine Receptors: The Contribution of σ -Hole Interactions. *ChemPhysChem* **2018**, 19, (22), 3069-3083.
32. Laurence, C.; Brameld, K. A.; Graton, J.; Le Questel, J.-Y.; Renault, E., The pKBHX Database: Toward a Better Understanding of Hydrogen-Bond Basicity for Medicinal Chemists. *Journal of Medicinal Chemistry* **2009**, 52, (Copyright (C) 2016 American Chemical Society (ACS). All Rights Reserved.), 4073-4086.
33. Graton, J.; Wang, Z.; Brossard, A.-M.; Goncalves, M. D.; Le, Q. J.-Y.; Linclau, B., An unexpected and significantly lower hydrogen-bond-donating capacity of fluorohydrins compared to nonfluorinated alcohols. *Angew Chem Int Ed Engl* **2012**, 51, (Copyright (C) 2016 U.S. National Library of Medicine.), 6176-80.
34. Graton, J.; Compain, G.; Besseau, F.; Bogdan, E.; Watts, J. M.; Mtashobya, L.; Wang, Z.; Weymouth-Wilson, A.; Galland, N.; Le Questel, J. Y., Influence of Alcohol β -Fluorination on Hydrogen-Bond Acidity of Conformationally Flexible Substrates. *Chemistry—A European Journal* **2017**, 23, (12), 2811-2819.
35. Ceron-Carrasco, J. P.; Jacquemin, D.; Graton, J.; Thany, S.; Le Questel, J.-Y., New Insights on the Molecular Recognition of Imidacloprid with *Aplysia californica* AChBP: A Computational Study. *Journal of Physical Chemistry B* **2013**, 117, (Copyright (C) 2016 American Chemical Society (ACS). All Rights Reserved.), 3944-3953.

36. Shinada, N. K.; de Brevern, A. G.; Schmidtke, P., Halogens in Protein–Ligand Binding Mechanism: A Structural Perspective. *Journal of Medicinal Chemistry* **2019**, 62, (21), 9341-9356.

Journal Pre-proofs

Conformation and structural features of diuron and irgarol: insights from quantum chemistry calculations.

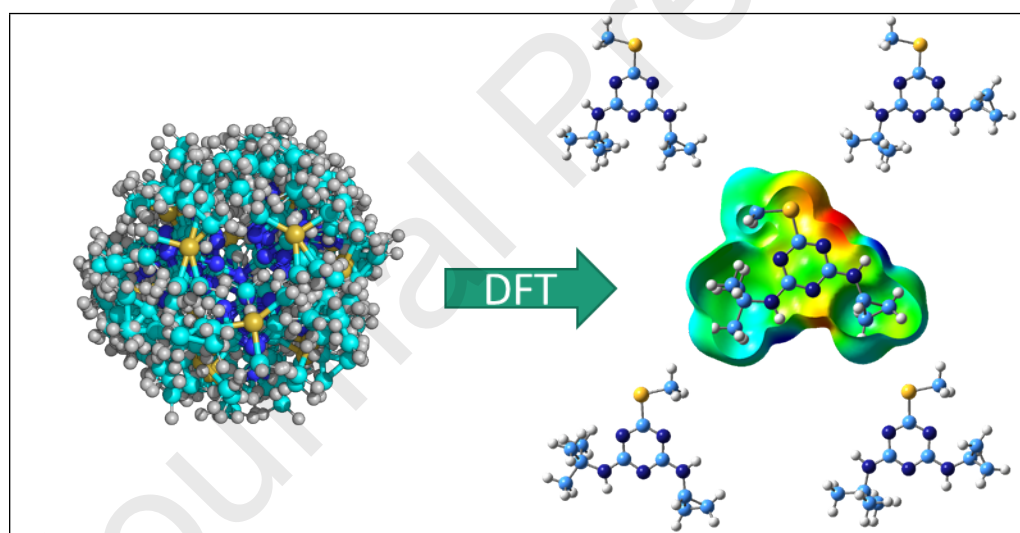
Zakaria Bouchouireb,^[a] Rossana Sussarellu,^[b] Sabine Stachowski-Haberkorn,^[b] Jérôme Graton,

^[a] Jean-Yves Le Questel* ^[a]

^[a] Nantes Université, CNRS, CEISAM, UMR 6230, F-44000 Nantes, France

^[b]Ifremer, BE-LEX, F-44300, Nantes France.

Graphical abstract



quantum chemistry calculations.

Zakaria Bouchouireb,^[a] Rossana Sussarellu,^[b] Sabine Stachowski-Haberkorn,^[b] Jérôme Graton,

^[a] Jean-Yves Le Questel* ^[a]

Highlights

- Diuron and irgarol structural features have been investigated by quantum chemistry (DFT) calculations and analyses of crystal structures retrieved from the Cambridge Structural Database (CSD) and the protein data bank (PDB)
- The effect of the surroundings have been taken into account in the calculations using the SMD model for water
- Molecular electrostatic potential calculations allowed to bring to light and rank the potential intermolecular interaction sites of the two biocides according to their conformation
- The potential of interaction of irgarol is found to be much more sensitive to the conformational preferences than the one of diuron

quantum chemistry calculations.

Zakaria Bouchouireb,^[a] Rossana Sussarellu,^[b] Sabine Stachowski-Haberkorn,^[b] Jérôme Graton,

^[a] Jean-Yves Le Questel* ^[a]

^[a] *Nantes Université, CNRS, CEISAM, UMR 6230, F-44000 Nantes, France*

^[b] *Ifremer, BE-LEX, F-44300, Nantes France.*

*Corresponding authors:

Jean-Yves Le Questel: jean-yves.le-questel@univ-nantes.fr

Tel :(+33)(0)2 51 12 55 63

Please find below as required the list of authors of this work and their contribution in the submitted work

CRedit authorship contribution statement

Zakaria Bouchouireb: investigation, writing—review and editing

Rossana Sussarellu : Conceptualization, writing—review and editing, project administration, funding acquisition.

Sabine Stachowski-Haberkorn : Conceptualization, writing—review and editing, project administration, funding acquisition.

Jérôme Graton : Conceptualization, methodology, formal analysis, investigation, writing—original draft preparation, writing—review and editing, supervision.

Jean-Yves Le Questel : Conceptualization, methodology, formal analysis, writing—original draft preparation, writing—review and editing, supervision.

Journal Pre-proofs

Declaration of interests

The authors declare that they have no known competing financial interests or personal relationships that could have appeared to influence the work reported in this paper.

The authors declare the following financial interests/personal relationships which may be considered as potential competing interests:

Journal Pre-proofs